There is consistency between this ^{31}P junction point data and the previous ^{13}C, segmental motion data.[13,14] For the segmental motion in networks with $M_c > 2000$ the ^{13}C relaxation pattern showed little network influence as evidenced by the close resemblance to the ^{13}C relaxation in long linear chains. This threshold is also shown in the ^{31}P line shapes and $T_{1\rho}^P$ of this work in that the M_c 425 and M_c 2000 networks show definite limitations to motion at full swell; i.e., the network chain constrains the cross-link motion. Even though we were unable to observe the high λ case for M_c 3000, it is clear from Figure 4 that little line-shape change will ensue with higher λ but the $T_{1\rho}^P$ would be of keen interest.

The origin of junction mobility is from the segmental motion and the interrelationship between the two is a topic of basic interest in understanding real networks. Further experiments in which simple extension of networks is followed by ^{31}P NMR are in progress. Comparison of dielectric measurement, ^{13}C NMR relaxation, and ^{31}P NMR relaxation on this system of networks shows that the ^{13}C $T_{1\rho}$ minimum is near the T_g from DSC and dielectric relaxation but that the ^{31}P junction point motion of the unswollen polymers begins at a much higher temperature than the segmental T_g. This strongly suggests coupling between the junction point motion and segmental motion suffers a lag, presumably because of the anchoring effects of multiple chains emerging symmetrically from each junction point.

In assigning particular motions to the large and rapid change in $T_{1\rho}^P$ with linear swell ratio (Figure 1), it is of interest to compare the changes in $T_{1\rho}^P$ with temperature in the unswelled networks.[14,22] Between room temperature and 310 K $T_{1\rho}^P$ for the M_c 3000 sample increases by only 1 order of magnitude. That swelling in toluene by a linear swelling ratio of only 1.5 increases by $T_{1\rho}^P$ 3 orders of magnitude dramatizes the motional freedom or rotational isomeric states made accessible by solvent. These differences should be theoretically calculable and could reflect a number of factors including inter- and intrachain limitations on available rotational isomeric states in networks.

In summary, this work shows that ^{31}P NMR is a powerful tool for examining the specific motion of the junction point in the networks. $T_{1\rho}^P$ is very sensitive to M_c, swell ratio, and defects in the network. $T_{1\rho}^P$ changes by several orders of magnitude between $\lambda = 1$ and 1.5 for M_c 3000 but hardly changes for M_c 425. ^{31}P line shapes for $M_c \leq 2000$ at maximum swell reflect the constraints placed on the junction point by the network chains. These orientational mobility results are in agreement with previous theories of Erman predicting linear variation of log (mobility) with λ within the range studied.[11]

Acknowledgment. We are grateful to Professor Burak Erman for his interest and guiding insights in this work.

Registry No. (PO)(tris(4-isocyanatophenyl) thiophosphate) (copolymer), 115678-76-7; (PPO)(tris(4-isocyanatophenyl) thiophosphate) (copolymer), 115678-77-8.

References and Notes

(1) Candau, S.; Bastide, J.; Delsanti, M. *Adv. Polym. Sci.* **1982**, *44*, 27.
(2) Nishi, T. *J. Polym. Sci., Polym. Phys. Ed.* **1974**, *12*, 685.
(3) Muncie, G. C.; Jonas, J.; Rowland, T. J. *J. Polym. Sci., Polym. Chem. Ed.* **1980**, *18*, 1061, and references therein.
(4) Folland, R.; Charlesby, A. *Polymer* **1979**, *20*, 211, and references therein.
(5) Cohen-Addad, J. P.; Domaro, M.; Herz, J. *J. Chem. Phys.* **1982**, *76*, 2744; Cohen-Addad, J. P.; Viallat, A.; Huchot, P. *Macromolecules* **1987**, *20*, 2146.
(6) Jacobi, M. M.; Stadler, R.; Gronski, W. *Macromolecules* **1986**, *19*, 2884.
(7) Gronski, W.; Stadler, R.; Jacobi, M. M. *Macromolecules* **1984**, *17*, 741.
(8) Dubault, A.; Deloche, B.; Herz, J. *Macromolecules* **1987**, *20*, 2096, and references therein.
(9) Doskocilova, D.; Schneider, B.; Jakes, J. *Polymer* **1980**, *21*, 1185.
(10) Jarry, J. P.; Erman, B.; Monnerie, L. *Macromolecules* **1986**, *19*, 2750.
(11) Erman, B.; Monnerie, L. *Macromolecules* **1986**, *19*, 2745.
(12) Dickinson, L. C.; Morganelli, P.; Chu, C.-W.; Petrovic, Z.; Chien, J. C. W.; MacKnight, W. J. *Macromolecules* **1988**, *21*, 338.
(13) Dickinson, L. C.; Morganelli, P. L.; MacKnight, W. J.; Chien, J. C. W. *Makromol. Chem., Rapid Commun.* **1987**, *8*, 425.
(14) Dickinson, L. C.; Chien, J. C. W.; MacKnight, W. J. *J. Polym. Sci., Polym. Phys. Ed.*, in press.
(15) MacKnight, W. J.; Petrović, Z. S., to be submitted for publication.
(16) McBrierty, V. J.; Douglass, D. C. *J. Magn. Reson.* **1970**, *2*, 352.
(17) Mehring, M. *High Resolution NMR in Solids*, 2nd ed.; Springer-Verlag: New York, 1983; pp 260–265.
(18) Wemmer, D. E. Ph.D. Thesis, University of California, Berkeley, 1979.
(19) Spiess, H. W.; Grosescu, R.; Haeberlen, V. *Chem. Phys.* **1974**, *6*, 226.
(20) Schmidt, C.; Blümich, B.; Weting, S.; Kaufman, S.; Speiss, M. W. *Ber. Bunsen-Ges. Phys. Chem.* **1987**, *91*, 1141.
(21) English, A. D.; Dybowski, C. R. *Macromolecules* **1984**, *17*, 446.
(22) Dickinson, L. C.; Chien, J. C. W.; MacKnight, W. J., to be submitted for publication.

Small-Angle Neutron Scattering of Cross-Linked Polystyrene Networks

Hwai-Min Tsay and Robert Ullman*

Department of Nuclear Engineering and Macromolecular Research Center, University of Michigan, Ann Arbor, Michigan 48109. *Received November 20, 1987; Revised Manuscript Received April 8, 1988*

ABSTRACT: Small-angle neutron scattering experiments have been performed on polystyrene networks labeled with deuterium. Changes in molecular dimensions of the polymer chains upon swelling and upon stretching in the rubbery state were derived from these measurements. The experimental observations were compared with predictions from classical theories, and areas of agreement and disagreement were discussed.

Introduction

The elasticity of rubbery materials results from the uncoiling of flexible molecular chains in the rubber network. Theoretical models of this phenomenon relate macroscopic variables such as the modulus of elasticity, thermodynamics of deformation, and swelling in solvents to the elongation of these molecular chains. Only in the past 15 years with the development of small angle neutron scattering (SANS) has it become possible to make direct measurements of macromolecular dimensions. By com-

0024-9297/88/2221-2963$01.50/0

paring experimental results on rubbery materials with predictions from the theory, it is now possible to choose among different theoretical models of rubber elasticity.

A rubber network is a giant macromolecule in which wormlike flexible polymer chains are connected at cross-link junction points. The junctions move with the macroscopic deformation of the specimen, while monomer units between the junctions rearrange depending on the positions of the junctions. In the classical model, the time-average distances between cross-link junctions are assumed to which deform affinely in the macroscopic coordinates. The model divides into several subclasses, the fixed junction network,[1,2] the phantom network,[3-6] and the Flory–Erman model.[7-9] In the fixed junction model, the cross-link junctions are fixed in space. In the phantom network, the polymer chains act as elastic springs and the junctions fluctuate in accordance with the theory of Brownian motion. It follows from the theory that the fluctuations are independent of the extent of deformation, and, therefore, though the average distances between junctions deform affinely, the root-mean-squared distances, which include fluctuations, do not. The fluctuations are, in fact, quite large, and the results predicted by the theory show very much less chain deformation than would be found in a network in which the junctions are immobile. The Flory–Erman model is intermediate between those two and depending on additional parameters may approach one or the other. It yields chain deformations closer to the fixed junction network at small macroscopic deformations but approaches those of the phantom network at large deformations.

There is another view of network uncoiling which takes into account junction rearrangement and its dependence on network topology and entanglement structure.[10-13] In this picture, a path in chain space which passes through a large number of cross-links will, in the limit of an infinitely long chain, deform affinely. However, short portions of the path will not necessarily do so, since elastic forces connecting topologically neighboring cross-link junctions are greater than indirect forces between geometrically neighboring junctions which are topologically remote. The deviation from affine deformation results from junction rearrangement which is itself restricted by network entanglements and repulsive interactions. These effects are very sensitive to the polymer concentration at the moment of cross-linking.

The centroidal radius of gyration of polymer chains can be extracted from a SANS measurement, and when distances between chain ends are perturbed by deforming the sample, the radius of gyration changes accordingly. This provides a direct and, in principal, unambiguous method of checking the theories with experiment.

If a polymer is cross-linked in bulk and deformed without swelling, there is no difficulty in defining a reference state with which chain dimensions in a deformed polymer can be compared. The reference state is the undeformed bulk polymer. If cross-linking takes place in solution and/or deformation occurs because of swelling, the choice of a reference state is no longer clear.[9,14] Comparison between theory and experiment is consequently uncertain. The problem will be analyzed in more detail further in this paper.

The theory of rubber elasticity is usually formulated for end-linked polymer chains. In fact, real rubbers are rarely end-linked but contain randomly distributed cross-links. Most SANS studies have been performed with end-linked networks. We have chosen to investigate randomly cross-linked networks even though data gathered on these systems is more difficult to interpret. In our experiments, each distinguishable polymer chain in the network has only a few cross-links, which is a case intermediate between an end-linked molecule and one in a network in which the polymer chain has very many cross-links and therefore must deform affinely.

Scattering Equations

The SANS investigations have been carried out on networks containing both protonated and deuteriated polymer. Some specimens have been uniaxially stretched and others swollen by a solvent. The scattering intensities were obtained from the number of counts on an area detector and corrected for transmission and incoherent background. The coherent elastic scattering $I(\mathbf{q})$ can be split into two parts, $I_s(\mathbf{q})$ which depends only on the internal geometry of the polymer chains and $I_t(\mathbf{q})$ which depends on both intra- and interchain geometry.[15-17] To be specific, these are

$$I(\mathbf{q}) = I_s(\mathbf{q}) + I_t(\mathbf{q}) \tag{1a}$$

$$I_s(\mathbf{q}) = (a_H - a_D)^2 x(1-x) N_p n^2 S_s(\mathbf{q}) \tag{1b}$$

$$I_t(\mathbf{q}) = (a_D x + a_H(1-x) - a_s)^2 N_p n^2 S_t(\mathbf{q}) \tag{1c}$$

In these equations, a_H and a_D are scattering lengths of a protonated (H) and deuteriated (D) monomer, respectively, and a_s is the scattering length of the solvent adjusted for the difference in volume between a solvent molecule and a monomer unit in the polymer chain. N_p is the number of polymer molecules in the specimen, n is the degree of polymerization of both protonated and deuteriated polymers, and x is the mole fraction of deuteriated polymer. Equations 1b and 1c apply to systems where the H and D polymers have the same degree of polymerization. The wave vector $\mathbf{q}$ equals $(2\pi/\lambda')(\mathbf{k} - \mathbf{k}_0)$ where $\mathbf{k}_0$ and $\mathbf{k}$ are unit vectors in the direction of the incident and scattered neutron beams. λ' is the neutron wave length. The magnitude of $\mathbf{q}$, designated as q, equals $(4\pi/\lambda')\sin(\theta/2)$, with the scattering angle, given by $\cos\theta = \mathbf{k}\cdot\mathbf{k}_0$. $S_s(\mathbf{q})$ and $S_t(\mathbf{q})$ are given by

$$S_s(\mathbf{q}) = (1/n^2)\sum_{i,j} \langle \exp(i\mathbf{q}\cdot\mathbf{r}_{ij}) \rangle \tag{2a}$$

$$S_t(\mathbf{q}) = (1/n^2 N_p) \sum_{\substack{i,j \\ \mathrm{M,N}}} \langle \exp(i\mathbf{q}\cdot\mathbf{r}_{ij}) \rangle \tag{2b}$$

In eq 2a, $\mathbf{r}_{ij}$ is a vector connecting monomer i to monomer j within the same chain. In eq 2b, $\mathbf{r}_{ij}$ connects monomer i on chain M to monomer j on chain N. An ensemble average is indicated by the angle bracket.

A polymer network is a single giant macromolecule. For the purpose of distinction, the words intra- and intermolecular will be used to refer to monomer pairs which, before cross-linking, were on the same or different molecules, respectively.

Equations 1a through 1c were derived for an incompressible system, in which density fluctuations are negligible. In this system, $S_t(\mathbf{q})$ and $I_t(\mathbf{q})$ are zero for a one component bulk polymer. $I_t(\mathbf{q})$ is also equal to zero if $a_s = a_D x + a_H(1-x)$. $I_s(\mathbf{q})$ vanishes if x is zero or one, and, accordingly, if the polymer contains only a single isotopic (H or D) species, the only scattering is given by $I_t(\mathbf{q})$ alone. $I_t(\mathbf{q})$ is sometimes referred to as the "total" scattering term and is what would be measured in an X-ray or light scattering investigation.

The scattering from an isotropic specimen is independent of azimuthal angle, and it is easy to show that

$$[I_s(\mathbf{q})]^{-1} = \mathrm{const}[1 + q^2 R_g^2/3 + O(q^4)] \tag{3a}$$

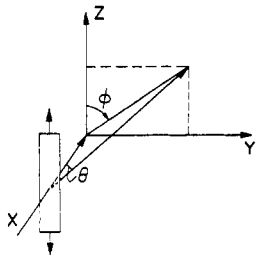

Figure 1. Schematic diagram of neutron scattering from uniaxially oriented specimens. The neutron beam is in the negative x direction, sample orientation is parallel to the z axis, θ is the scattering angle, and ϕ is the azimuthal angle.

where R_g^2, the mean squared radius of gyration, is obtained from a linear plot of $[I_s(\mathbf{q})]^{-1}$ versus q^2, at low q. Thus

$$R_g^2 = 3(\text{slope}/\text{intercept}) \tag{3b}$$

The scattering from stretched samples depends on the geometric arrangement of the experiment. Consider a uniaxially oriented specimen with the principal axis parallel to the z axis, the incident neutron beam in the (negative) x direction, and the detector in the yz plane. This is shown in Figure 1, in which the azimuthal angle, ϕ, is measured clockwise from the z axis. For small scattering angles, the wave vector, $\mathbf{q}$, can be considered to lie in the plane of the detector.

For a stretched specimen fixed in the geometry of Figure 1, scattering depends on both θ and ϕ. A plot of $[I(\mathbf{q})]^{-1}$ versus q^2 at an azimuthal angle ϕ yields a projection of the radius of gyration in the ϕ direction. In analogy with eq 3b

$$R_\phi^2 = 3(\text{slope}/\text{intercept}) \tag{4}$$

For our purpose, only $\phi = 0$ and 90° will be considered, where $R_\parallel$ refers to $\phi = 0$ and $R_\perp$ to $\phi = 90°$. For the unoriented sample, $R_\parallel = R_\perp = R_g$. In general

$$R_g^2 = (R_\parallel^2 + 2R_\perp^2)/3 \tag{5}$$

Molecular Dimensions and Network Deformation

If a rubber is prepared by cross-linking at the chain ends in the bulk state and deformed by stretching

$$R_\parallel^2 = 0.5R_g^{\circ 2}[1 + \lambda^2] \tag{6a}$$

in the fixed junction network and

$$R_\parallel^2 = 0.5R_g^{\circ 2}[1 + \lambda^2 - (2/f)(\lambda^2 - 1)] \tag{6b}$$

in the phantom network.[18] In these equations, R_g° is the radius of gyration in the bulk undeformed cross-linked polymer. λ is equal to L/L_0 where L_0 is the length of the specimen before stretching and L, its length after stretching. f is the network functionality. Volume changes of rubber are usually small when stretched, and the corresponding relations for $R_\perp$ are obtained by substituting $\lambda^{-1/2}$ for λ in eq 6a and 6b.

The equations for deformation of polymer chains in a network swollen by a solvent are of the same form as eq 6a and 6b.

$$R_g^2 = 0.5R_g^{*2}[1 + \lambda^2] \quad \text{(fixed junction network)} \tag{7a}$$

$$R_g^2 = 0.5R_g^{*2}[1 + \lambda^2 - (2/f)(\lambda^2 - 1)] \quad \text{(phantom network)} \tag{7b}$$

Here, λ is the linear expansion of the gel equal to $(V/V^0)^{1/3}$ where V^0 and V are the volumes of the specimen before and after swelling, respectively. The difference, if any, between eq 6 and 7 is that R_g^*, the radius of gyration in the reference state, may not be equal R_g^0, the radius of gyration of the cross-linked bulk polymer.

The theories of rubber elasticity provide predictions of the ratio of the radius of gyration of the swollen rubber relative to an appropriately chosen reference state, and the choice of the reference state is uncertain. For a polymer cross-linked in bulk, two possible choices are immediately evident, first, the radius of gyration in the cross-linked bulk polymer, and second, the radius of gyration of the polymer in solution at the same concentration as the polymer in the gel. A third possibility, for polymer cross-linked in solution, is to choose the reference state to be that of the polymer in the cross-linked gel before swelling or deswelling. This last is not pertinent to our experiments, since all cross-linking was carried out on the bulk polymer.

If a network is prepared by cross-linking polymer chains more or less randomly, the final network will be composed of the original molecules, each of which contains one or more cross-links. Consider the parallel projection of the radius of gyration, of a chain in the stretched network. It may be written

$$R_\parallel^2 = \sum P(k)R_\parallel^2(k) \tag{8a}$$

where $R_\parallel(k)$ is the value of $R_\parallel$ of a molecule with k cross-links and $P(k)$ is the probability of having k cross-links. In a loosely cross-linked system in which k is much less than n and crosslinking is random

$$P(k) = x^k e^{-x}/k! \tag{8b}$$

It is easy to show that $x = \bar{k}$, the average number of cross-links per chain. $R_\parallel^2(k)$ and $R_\perp^2(k)$ have been calculated previously for multilinked chains for both the phantom network and fixed junction networks.[19]

$$R_\parallel^2(k) = R_g^{02}[1 + (\lambda^2 - 1)F(k)/(k + 1)^3] \tag{9a}$$

$$F(k) = (k - 1)(2k^2 + 6k + 1)/2 \quad \text{(fixed junction network)} \tag{9b}$$

$$F(k) = (k^3 - k) + (f - 2)(4k + 1)(k - 1)/2f - G(f) \quad \text{(phantom network)} \tag{9c}$$

$$G(f) = [12(f - 1)/f(f - 2)](T_1 + 2T_2 + T_3) \tag{9d}$$

$$T_1 = 1 - (f - 1)^{1-k} \tag{9e}$$

$$T_2 = (k - 2) + (1 - (f - 1)^{1-k})/(f - 2) \tag{9f}$$

$$T_3 = (k - 2)(k - 3)/2 + [(k - 3)(f - 1) - (k - 2) + (f - 1)^{3-k}]/(f - 2)^2 \tag{9g}$$

Equations 9a through 9g are only valid for k equal to or greater than 2, since a chain with a single cross-link is not deformed at equilibrium in a stretching experiment. Similarly, in a swollen gel, deformation of a chain with a single cross-link arises from solvent–polymer interactions only; no network forces are active.

Fluctuations of neighboring subchains are coupled in a multilinked network since a positive fluctuation in one subchain corresponds, in part, to a negative fluctuation in the neighboring subchain. As a consequence, $R_\parallel^2(k)$ is the same for the phantom and fixed junction networks in the limit of large k. Equations for $R_\perp(k)$ are obtained from those for $R_\parallel(k)$ by replacing λ by $\lambda^{-1/2}$, assuming that there is no volume change upon stretching.

The radius of gyration and its projections in different azimuthal directions are calculated from the initial decay of $I_s(\mathbf{q})$ with $\mathbf{q}$ as described above. The decay of $I_t(\mathbf{q})$ with $\mathbf{q}$ yields a correlation length. The correlation length is a measure of the geometric range over which the presence of a given chain molecule affects the concentration of

neighboring molecules. According to a model proposed by Edwards[20]

$$I_t(\mathbf{q}) \approx (1 + q^2l^2)^{-1} \quad (10)$$

and l, the correlation length, is obtained from a plot of $I_t(\mathbf{q})^{-1}$ versus q^2.

Experimental Section

Preliminary Experiments. Our first experiments were carried out on networks prepared from homogeneous blends of polystyrene (PSH) and poly(deuteriostyrene) (PSD) by γ-radiation from a ^{60}Co source. All specimens were irradiated in evacuated Pyrex containers with a total dosage of 1000 Mrad. Before the samples were exposed to air, they were heated at 80 °C for 48 h to terminate trapped free radicals. The samples had a mean cross-link density of 2.3, and the cross-link density was found to be higher in PSH than in PSD. The isotope effect introduces difficulties in interpretation of experiments. In addition, the time required to prepare networks of adequate cross-link density was between 3 and 9 months. The isotope effect and slow reaction rate persuaded us to search for another cross-linking procedure, and the irradiation experiments were abandoned.

Cross-Linking Procedure and Analysis. Sulfonyl azides react with aromatic hydrocarbons[21-23] upon heating, by the following reactions

$$RSO_2N_3 \xrightarrow{\Delta} RSO_2N^\bullet + N_2$$

$$RSO_2N^\bullet + R'\langle\bigcirc\rangle \longrightarrow RSO_2NH\langle\bigcirc\rangle R'$$

Though reaction can take place with both aliphatic and aromatic H atoms, most if not all of the reaction is with the aromatic ring of polystyrene. It is well-known that disulfonyl azides will cross-link polystyrene,[24] and this is what was done to prepare the cross-linked samples studied in this investigation.

The cross-linking agent *m*-benzenedisulfonyl azide (BDSA) was prepared by reacting *m*-benzenedisulfonyl chloride with sodium azide. BDSA was codissolved with PSH and PSD and freeze-dried. PSH was purchased from Pressure Chemical and had a molecular weight of 1.0×10^5 and a polydispersity index (M_w/M_n) of 1.06. PSD was purchased from the Polymer Laboratories with a molecular weight of 1.1×10^5 and a polydispersity of 1.05.

The uniformly mixed dried powder of PSH, PSD, and BDSA was compacted in a stainless steel mold under vacuum at 155 °C and 1000 psi for an hour. The samples prepared for the swelling experiments were circular disks, 1.3 cm in diameter and approximately 0.1 cm thick. Dumbbell-shaped samples were used in the stretching experiments. The central sections of the latter were 3.17 cm long and 1.27 cm across. They were also approximately 0.1 cm thick.

In all cases, the cross-linking was carried out in bulk polymer. In our calculation of cross-linking efficiency, it is assumed that no cross-links are wasted in intramolecular reaction. This assumption is imperfect but more nearly correct in a bulk polymer than in a system containing solvent.

In a randomly cross-linked system beginning with a well-characterized polymer, the average number of cross-links per chain in both the gel and sol phases is a known function of the sol/gel ratio. Equations given by Charlesby[25] taken together with known stoichiometry were used to calculate the efficiency of the cross-linking reaction. Since the sol concentrations of the networks prepared for the scattering experiments were low, networks specially prepared at lower cross-link levels and therefore higher sol concentrations were used to determine the completeness of the sulfonyl azide reaction with the polymer. The cross-linking efficiency determined in this manner was 0.58. The cross-link densities of the networks used in the scattering experiments were recalculated by multiplying the stoichiometric cross-link densities, assuming 100% reaction, by $0.58(2 - g)$ where g is the gel fraction.

Cross-Linking Selectivity. If there were a strong isotope selectivity in the cross-linking reaction, the PSH/PSD ratio in the network would become a function of time as the reaction proceeds. Large scale inhomogeneities thereby generated would make interpretation of results virtually impossible. The selectivity factor was determined by Fourier transform infrared spectroscopy based on relative concentrations of C–H and C–D in the sol fraction. The C–H and C–D stretching frequencies, 2820–3130 and 2020–2340 cm^{-1}, respectively, were used for the measurement. The actual PSH and PSD concentrations were determined from the infrared absorbance by calibration with standard PSH–PSD solutions. From this, the ratio of reaction of BDSA and PSD to that with PSH was found to be 1.15. For our purposes, this is sufficiently close to unity that isotopic selectivity could be subsequently ignored.

All samples were clear glasses before swelling or stretching. Those with the highest concentration of cross-linking agent contained small bubbles from nitrogen produced during the sulfonyl azide–hydrocarbon reaction. As far as we could tell from scattering measurements, these bubbles had no effect on the scattering pattern.

Preparation of Swollen Gels and Stretched Samples. Cross-linked polystyrene networks were fully swollen in toluene-d_8. Many of these were partially deswollen by evaporation and then sealed in air-tight containers and allowed to equilibrate for at least a week before SANS measurement. The polystyrene networks used to study the effect of temperature on swelling were fully swollen in cyclohexane-d_{12}. In all cases the small fraction of sol was extracted by repeated soaking in an excess of swelling agent.

Specimens of PSD–PSH blends were molded into a dumbbell shape and then cross-linked. These were stretched slowly (5 mm/min) at 150 °C and allowed to relax under load for 10 min before quenching to room temperature. The extent of elongation was determined by measuring the ratio of the major axis of a fiduciary circle marked on the center of the sample after and before stretching. Sample thicknesses were recorded. The scattering measurements were performed weeks or months after deformation.

SANS Experiments. All SANS measurements were performed at the Oak Ridge National Laboratory on the 30-m SANS spectrometer at the high flux isotope reactor (HFIR). The wave length λ' of the neutrons was 4.75 Å, and the wavelength spread $\delta\lambda'/\lambda'$ equaled 0.06, full width at half-maximum. The scattering geometry was varied, the most important parameter of which was the sample–detector distance (SDD). Measurements were made at SDD's of 3, 7, and 16.5 m, with 7 m the most frequently used setting. The beam collimation was controlled by source and sample slits. In all experiments on swollen gels a sample slit of 1 cm was used, whereas a sample slit of 0.8 cm was adopted for the uniaxially stretched networks. Various source slits were used to ensure that all unscattered neutrons be captured by the beam stop in front of the detector.

The data analysis was carried out after the incoherent background was subtracted. This background was relatively small and estimated by using toluene/toluene-d_8 solutions as a reference. The scattering intensities of these solutions were independent of q and when plotted against the macroscopic incoherent cross section provided a basis for estimating incoherent scattering from the polymeric systems. The incoherent scattering from the polymer and the polymer gels was obtained from calculated macroscopic incoherent cross sections and interpolation on the calibration curve constructed from the above toluene mixtures.

Reliable scattering measurements were obtained for $0.006\ Å^{-1} \leq q \leq 0.16\ Å^{-1}$. The polymer chains had radii of gyration between 85 and 150 Å, and it is clear that experimental data at lower values of q than $0.006\ Å^{-1}$ are required for accurate determination of radii of gyration. In the absence of such data, errors of 10–20% are introduced.[26,27]

Our interest is not in absolute values of the radius of gyration but rather in values relative to a reference state. Errors in the ratio $R_g/R_g°$ are much lower than errors in R_g or $R_g°$ alone since many errors are systematic and in the same direction. The systematic errors in $R_g/R_g°$ are probably about 5%, an acceptable level in this investigation.

Determination of Chain Dimensions in Oriented Networks. Experimental difficulties are more pronounced in the determination of molecular dimensions from oriented polymer than from isotropic samples. The scattering from oriented specimens is a function of the azimuthal angle, ϕ, and either data are utilized over a narrow range of ϕ and errors are large or data are used at all ϕ, with the assumption that the functional de-

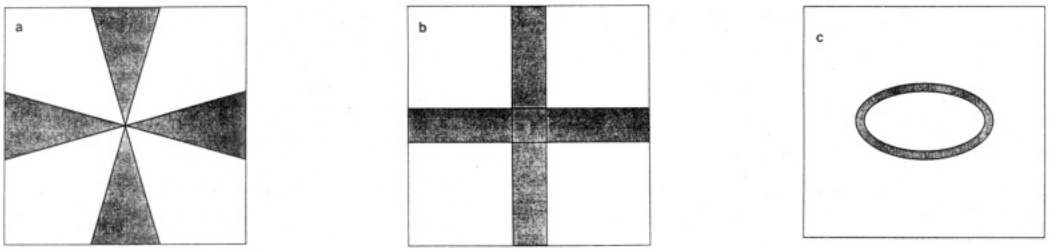

Figure 2. Schematic drawings of the different methods of extracting parallel and perpendicular contributions to the scattering from data collected on a two-dimensional detector: (a) SECTOR, (b) STRIP, and (c) ELLIPSE methods.

pendence of scattering on ϕ is known. In the latter method, there is a risk that the assumption is incorrect.

We have used three different techniques in analyzing our experiments on uniaxially oriented networks, two of which use data in a restricted range of ϕ and another which uses all the data. For identification, these are designated as SECTOR, STRIP and ELLIPSE methods. In parts a–c of Figure 2, drawings of a two dimensional detector are shown with shaded areas to indicate the range of data included in each of the methods.

Figure 2a shows a SECTOR of the detector centered at ϕ = 0° and 90°. At each value of q (constant distance from the center point of the detector), the intensity at ϕ = 0° is taken to be the average over the prescribed range of ϕ. The approximation is best, in principle, at small values of ϕ. However, too small an angle means too few counts and a large error. This is particularly serious at low q.

The STRIP method shown in Figure 2b takes data from a wider range of ϕ at low q, reducing some errors of the previous method. However, the change in ϕ with q may introduce a systematic error which can distort the result.

The ELLIPSE method is based on the assumption that, in uniaxial orientation as specified in Figure 1, lines of constant intensity fall on an ellipse centered on the detector. The ellipse shown in Figure 2c is an isointensity region. Summerfield and Mildner[28,29] have shown how a complete set of data from an area detector could be used for the analysis, thus drastically reducing experimental errors. Since, on theoretical grounds, one expects isointensity contours to be ellipsoidal at low q, the procedure has merit in determination of $R_\parallel$ and $R_\perp$ from scattering experiments.

A previously calibrated specimen of aluminum (Al-4), containing small voids, was used to obtain absolute intensities.[30] This was done by measuring the scattering from the aluminum standard under identical experimental conditions used for the scattering specimens. The absolute intensity of scattering from the polymer samples is also known at zero angle, and this provides an additional control of the quality of measurements. A discrepancy of 30% or so is a strong indication of a hidden error in the experiment. We have rejected data from three samples for this reason.

Experimental Results

Swollen Gels. Three series of gels were prepared. The first was composed of PSD/PSH networks in a molar ratio of 5:1, swollen in toluene-d_8. The PSD/PSH ratio was chosen so that the contrast factor of $I_t(q)$ vanished in these gels, and $I_s(\mathbf{q})$ and radii of gyration could be obtained directly. The second series used a PSD/PSH ratio of 5:3, and the swelling agent was cyclohexane-d_{12}. $I_t(q)$ vanished here also. The third series was composed of PSH networks in toluene-d_8. In this case $I_s(\mathbf{q})$ = 0, the scattering arose only from $I_t(\mathbf{q})$, and correlation lengths were derived therefrom.

Scattering patterns collected at different sample detector distances (SDD) cover different overlapping ranges of q. If these are properly calibrated, in our case by the porous aluminum standard, the scattering curves should overlap with possible minor corrections for instrumental resolution. Figure 3 shows the scattering of a PSD/PSH gel swollen in toluene-d_8 measured at three different SDD's and normalized. Agreement is satisfactory.

Figure 4 is a plot of $[I_s(\mathbf{q})]^{-1}$ versus q^2 (Zimm plot) of the same sample shown in Figure 3, based on data accumulated at SDD = 6.9 m. Radii of gyration from gels swollen in toluene-d_8 are given in Table I. They are presented as a ratio R_g/R_g° and R_g/R_g^s, since as described earlier, the ratios are known with better accuracy than

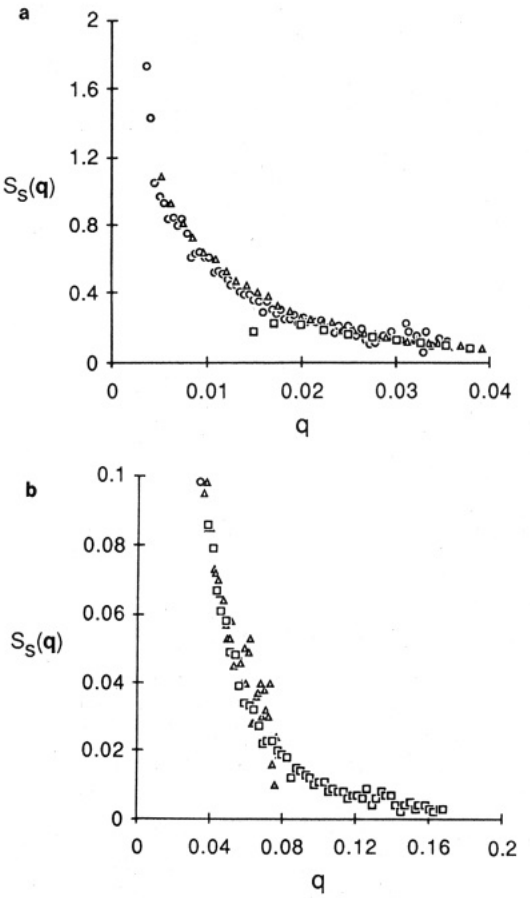

Figure 3. Plots of $S_s(\mathbf{q})$ versus q for a PSH/PSD network swollen in toluene-d_8 (c = 0.159 g/mL, $\bar{k}$ = 4.1): a, low q region; b, high q region. Data collected at three sample–detector distances: (○) 16.5 m, (△) 6.9 m, (□) 3 m.

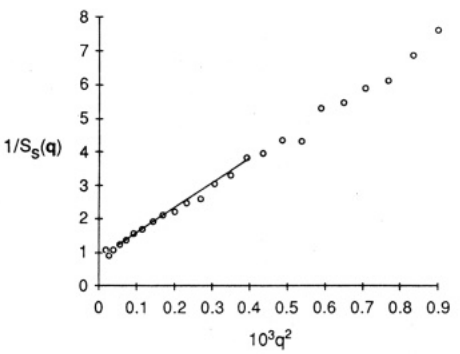

Figure 4. Plot of $1/S_s(\mathbf{q})$ versus q^2 for a PSH/PSD network swollen in toluene-d_8 (c = 0.159 g/mL, $\bar{k}$ = 4.1). A line of least-squares fit to the data is drawn to show the q region used to compute R_g.

Table I
Chain Deformation of Swollen Polystyrene Networks in Toluene

$\bar{k}$	c^a	λ	$R_g/R_g^{\circ\,b}$	$R_g/R_g^{\circ\,c}$	$R_g/R_g^{s\,d}$
3.1	0.100	2.192	1.622		1.355
3.1	0.123	2.045	1.523		1.293
3.1	0.169	1.840	1.494		1.300
3.1	0.247	1.621	1.372		1.230
3.1	0.508	1.275	1.247		1.183
4.1	0.135	1.983	1.814	1.692	1.552
4.1	0.159	1.878	1.666	1.640	1.444
4.1	0.364	1.425	1.434		1.325
4.1	0.377	1.408	1.393	1.398	1.291
5.2	0.183	1.792	1.599		1.400
5.2	0.184	1.788	1.700		1.490
5.2	0.185	1.785	1.715		1.503
5.2	0.277	1.561	1.485		1.344

[a] g of polymer/mL of gel. [b] Sample–detector distance = 6.9 m. [c] Sample–detector distance = 16.5 m. [d] R_g^s is the radius of gyration of uncross-linked polystyrene in toluene. $R_g^s/R_g^\circ = c^{-0.078}$. See ref 31.

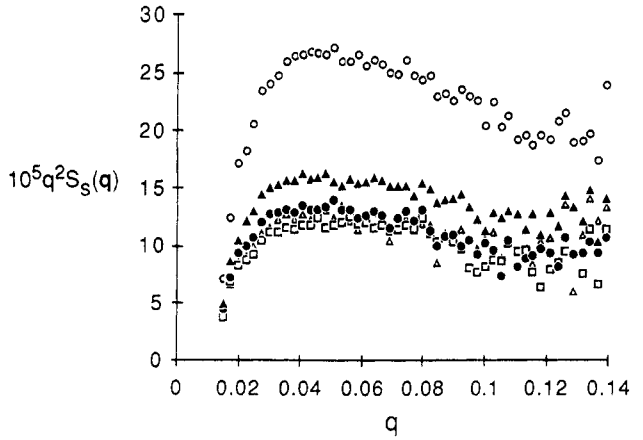

Figure 5. Kratky plots for a PSH/PSD network swollen in toluene-d_8 (SDD = 3 m; $\bar{k}$ = 4.1): (○) unswollen, (▲) c = 0.377 g/mL, (●) c = 0.364 g/mL, (□) c = 0.209 g/mL, (△) c = 0.159 g/mL.

absolute values. R_g° is the radius of gyration of the polymer chain in the network in the unswollen state. R_g^s is the radius of gyration of the uncross-linked polymer in solution where the polymer concentration is the same as that of the gel with which it is compared. R_g^s is calculated from results of King et al.,[31] who found $R_g^s = R_g^\circ c^{-0.078}$ for polystyrene of molecular weight 10^5 with toluene-d_8 as solvent.

Experimental data at low q yields the radius of gyration. At higher q, other characteristics of the polymer system are exhibited. An example of a typical experiment on a PSD/PSH gel in toluene-d_8 is shown in Figure 5. The results are presented in a Kratky plot, that is $q^2I_s(\mathbf{q})$ versus q. The shape of the plot is similar for all samples.

SANS measurements were conducted at different temperatures on PSD/PSH networks fully swollen in cyclohexane-d_{12}. R_g/R_g° values derived therefrom are given in Table II. The data cannot be represented as R_g/R_g^s as was done for gels swollen in toluene, since no measurements of radii of gyration of concentrated solutions of polystyrene in cyclohexane are available. However, Bauer and Ullman[32] show that molecular dimensions of a polymer of molecular weight 10^5 change by less than 5% within 10 °C of the Θ temperature (see Figure 1 of ref 32), and, according to Strazielle and Benoit[33] our PSD/PSH mixtures should have a Θ temperature of approximately 38 °C. Therefore, we shall treat R_g^s at 30 and 40 °C as equal to R_g°.

Table II
Chain Deformation of Fully Swollen Polystyrene Networks in Cyclohexane at Different Temperatures

$\bar{k}$	T, °C	c^a	λ	R_g/R_g°
3.1	60.5	0.264	1.586	1.209
3.1	50.5	0.323	1.483	1.202
3.1	40.5	0.347	1.448	1.191
3.1	30.5	0.370	1.417	1.113
3.1	20.5	0.392	1.390	1.092
4.1	60.5	0.320	1.488	1.257
4.1	50.5	0.353	1.439	1.185
4.1	40.5	0.397	1.384	1.215
4.1	30.5	0.454	1.324	1.143
4.1	20.5	0.479	1.300	1.156
5.2	60.5	0.383	1.401	1.281
5.2	50.5	0.451	1.326	1.219
5.2	40.5	0.501	1.281	1.207
5.2	30.5	0.561	1.233	1.168
5.2	20.5	0.579	1.220	1.195

[a] g of polymer/mL of gel.

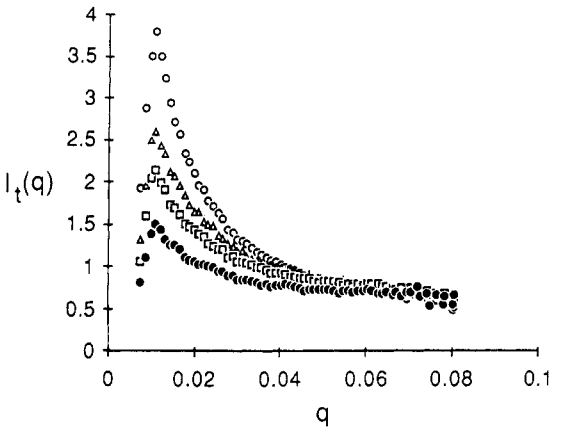

Figure 6. Plots of $I_t(\mathbf{q})$ versus q for PSH networks swollen in toluene-d_8 (SDD = 6.9 m; $\bar{k}$ = 4.1): (○) c = 0.119 g/mL, (△) c = 0.157 g/mL, (□) c = 0.189 g/mL, (●) c = 0.242 g/mL.

Pure PSH networks were swollen in toluene-d_8. In this case $I_s(\mathbf{q})$ equals zero, and correlation lengths can be derived from scattering function, $I_t(\mathbf{q})$. The scattering curves shown in Figure 6 have maxima at $\mathbf{q}$ approximately equal to 0.012 Å^{-1}. The Edwards model of polymer solutions[20] predicts a monotonically decrease in scattering intensity with increasing q. The scattering intensity from our gels decreased smoothly for q greater than 0.012 Å^{-1}, and the Edwards model was applied to scattering data at higher q, beginning at q = 0.014 Å^{-1}. $[I_t(\mathbf{q})]^{-1}$ was linear in q^2, and correlation lengths were calculated.

Uniaxially Stretched Networks. SANS measurements on uniaxially stretched PSH/PSD networks were performed. Typical results presented as Kratky plots are seen in Figure 7. The results are presented in Table III with calculations of $R_\parallel$ and $R_\perp$ made by the SECTOR, STRIP, and ELLIPSE methods. Errors are large, and, in our judgment, in part on the basis of the smoothness of results, the best representation is given by the STRIP method. This shall be used later to compare experiments with theoretical calculations. It should be recognized that any systematic error inherent in the STRIP method would lead to an overestimation of the anisotropy. Since the samples were only modestly oriented, the estimated systematic errors should be small.

Comparison of Experiments with the Phantom and Fixed Junction Network Swollen Gels—Radii of Gyration and Correlation Lengths. The swelling of polymer chains in cross-linked polystyrene networks can be compared with calculations on multilinked chains for

Table III
Chain Deformation of Uniaxially Stretched Polystyrene Networks

		$R_\parallel/R_g°$			$R_\perp/R_g°$		
$\bar{k}$	λ	ellipse	strip	sector	ellipse	strip	sector
3.1	1.210	1.112	1.129	1.118	0.979	0.950	0.937
3.1	1.436	1.230	1.194	1.234	0.984	0.939	0.981
3.1	1.682	1.329	1.244	1.278	0.917	0.918	0.934
3.1	1.875	1.341	1.272	1.261	0.939	0.916	0.949
4.1	1.216	1.139	1.126	1.150	0.957	0.960	0.970
4.1	1.449	1.268	1.258	1.237	0.964	0.905	0.889
4.1	1.585	1.320	1.301	1.386	0.950	0.873	0.882
4.1	1.887	1.586	1.413	1.473	1.031	0.863	0.922
5.2	1.137	1.230	1.118	1.182	0.972	0.970	1.047
5.2	1.210	1.159	1.141	1.197	0.962	0.928	1.006
5.2	1.447	1.344	1.262	1.355	0.914	0.881	0.920
5.2	1.619	1.382	1.347	1.418	0.885	0.859	0.886

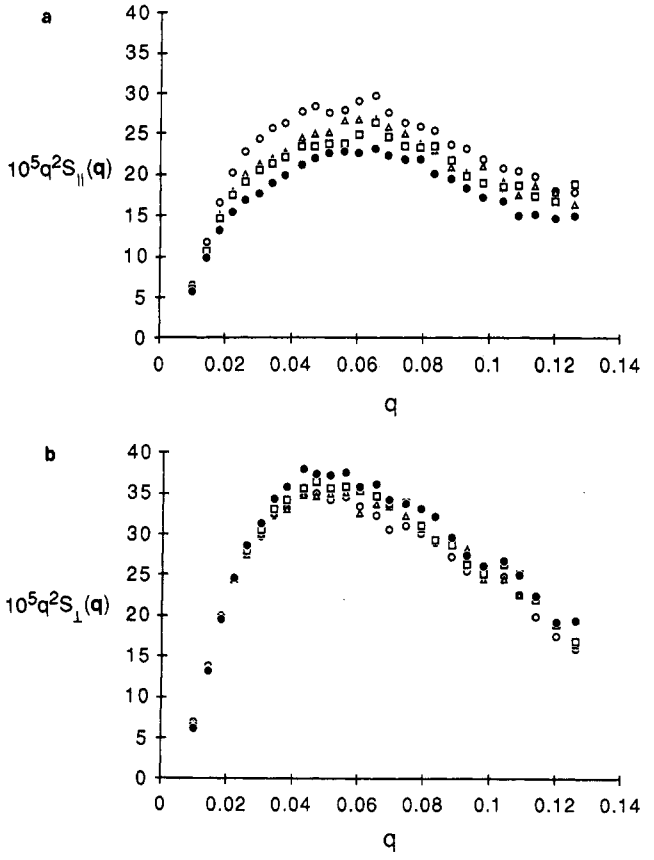

Figure 7. Kratky plots of the projection of scattering from stretched networks (SDD = 2.8 m; $\bar{k}$ = 4.1): (○) λ = 1.216, (△) λ = 1.449, (□) λ = 1.585, (●) λ = 1.887; a, parallel projection; b, perpendicular projection.

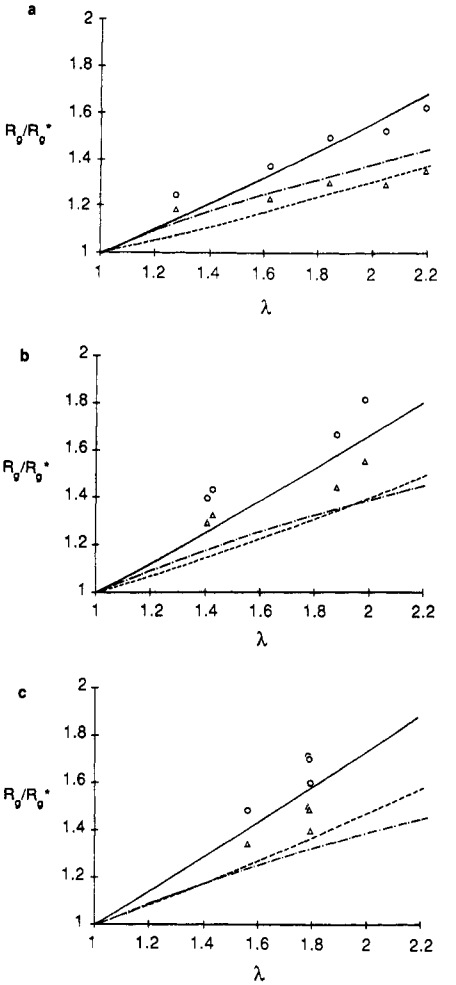

Figure 8. Plots of experimental values of R_g/R_g* versus for PSH/PSD networks swollen in toluene-d_8: a, $\bar{k}$ = 3.1; b, $\bar{k}$ = 4.1; c, $\bar{k}$ = 5.2; (○) $R_g* = R_g°$, (△) $R_g* = R_g^s$. Theoretical curves: —, fixed junction network: - - -, phantom network: ···, $R_g^s/R_g°$.

phantom network and fixed junction networks using eq 8a and 8b and eq 9a through 9g. Experimental results on PSH/PSD networks in toluene-d_8 are presented as $R_g/R_g°$ and R_g/R_g^s versus λ in parts a–c of Figure 8 together with calculated curves derived from the phantom network and fixed junction network models. In doing so, we reserve judgment as to whether $R_g°$ or R_g^s is a suitable reference state. The results from Table II on similar networks in cyclohexane-d_{12} are plotted as $R_g/R_g°$ versus λ (parts a–c of Figure 9).

Correlation lengths were computed from experiments on PSH networks in toluene-d_8. These are calculated from the scattering curves, shown in Figure 6 using the interval 0.014 Å $\leq q \leq$ 0.039 Å. A plot of log l versus log c, shown in Figure 10, is linear as is expected for polymer solutions which obey the usual scaling laws. The power law obtained from Figure 10 is $l = 10.57c^{-0.72}$. The theoretical prediction for a polymer solution in a good solvent is $l \sim c^{-0.8}$,[34] whereas several experiments on polymer solutions yielded results of $c^{-0.7}$.[31,34,35]

Uniaxially Stretched Networks. Values of $R_\parallel/R_g°$ and $R_\perp/R_g°$ given in Table III are compared with results based on the phantom network and fixed junction network in parts a–c of Figure 11. The experimental points on the figures are those obtained by the STRIP method.

Discussion of Results

Swollen Gels. Parts a–c of Figure 8 contain results on chain swelling relative to both the bulk polymer and the corresponding polymer solution. If the bulk polymer is taken as the reference state, chain expansion would appear to be greater than the fixed junction network and the

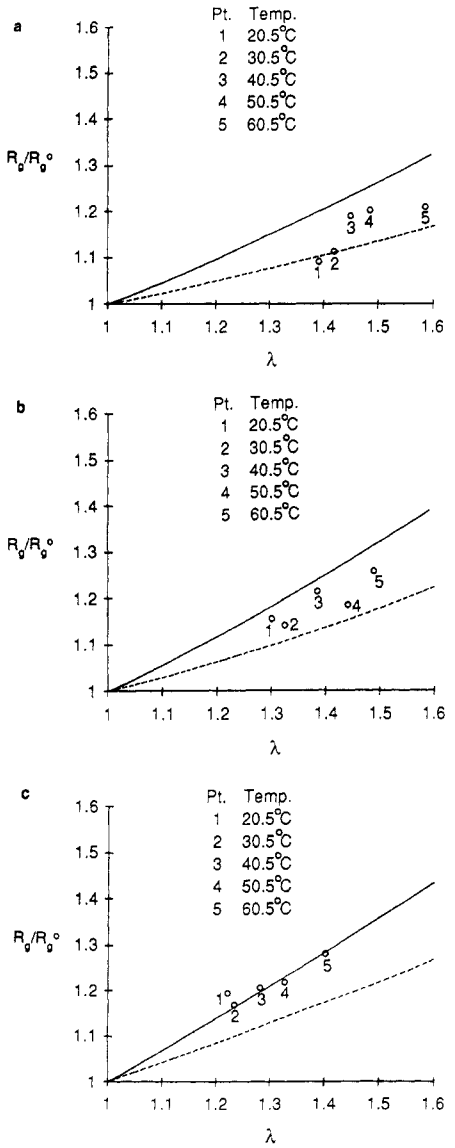

Figure 9. Plots of experimental values of $R_g/R_g°$ versus λ for PSH/PSD networks fully swollen in cyclohexane-d_{12} at different temperatures: a, $\bar{k}$ = 3.1; b, $\bar{k}$ = 4.1; c, $\bar{k}$ = 5.2. Theoretical curves: —, fixed junction network; - - -, phantom network. See Table II for gel concentrations.

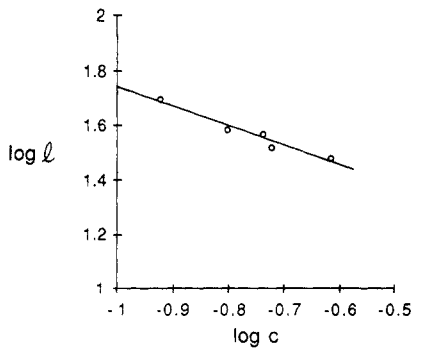

Figure 10. log–log plot of correlation length versus concentration for the PSH networks swollen in toluene-d_8.

latter, on theoretical grounds, provides an upper limit to the expected chain swelling. On the other hand, using the polymer solution as a reference state, the experiments fall in a range consistent with theoretical limits.

In parts a–c of Figure 12, R_g/R_g^s for networks swollen in toluene and $R_g/R_g°$ in cyclohexane are plotted together versus the linear swelling ratio. The points do scatter but fall roughly on lines which pass through the origin (1,1)

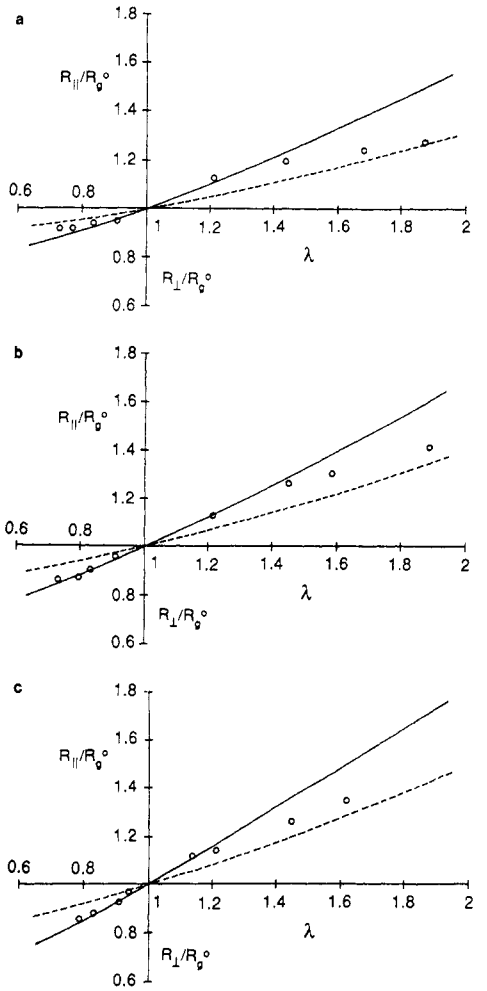

Figure 11. Plots of experimental values of $R_{\parallel}/R_g°$ and $R_{\perp}/R_g°$ versus λ for uniaxially stretched PSH/PSD networks: a, $\bar{k}$ = 3.1; b, $\bar{k}$ = 4.1; c, $\bar{k}$ = 5.2. Theoretical curves: —, fixed junction network; - - -, phantom network.

of the graphs. Admittedly the networks in cyclohexane and in toluene are not strictly comparable, owing to different degrees of swelling and to the variation of temperature in the cyclohexane experiment. Nevertheless, the figures provide substantial support for choosing R_g^s rather than $R_g°$ as a reference state for chain swelling.

Taking the data on R_g/R_g^s for PSD/PSH gels in toluene-d_8 and $R_g/R_g°$ in cyclohexane-d_{12} as appropriate measurements of chain swelling, we found results intermediate between the fixed junction and phantom networks models. In Erman's analysis of chain expansion,[9] the radius of gyration of the reference state is that at the time of cross-linking, which for our networks is the bulk polymer. Our results do not agree with the Erman theory if the radius of gyration in the unswollen network is taken as reference.

Our results show that $R_g/R_g°$ in toluene-d_8 is much greater than $R_g/R_g°$ in cyclohexane-d_{12} at comparable swelling. This illustrates the importance of solvent–polymer interactions on molecular dimensions, a contribution which is not taken into account in classical theories. If R_g^s is taken as the reference state, agreement between gels swollen in the good solvent (toluene) and the poor solvent (cyclohexane) is greatly improved. In our opinion, R_g^s is not an ideal reference point either. A better choice would require a more subtle analysis which takes into account both the driving force of polymer–solvent interactions and the elastic forces applied on the chain at cross-link junctions.

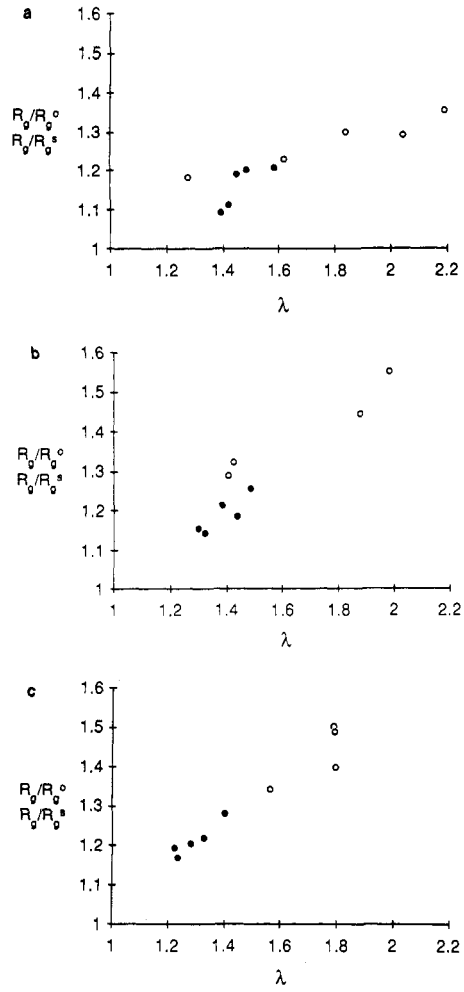

Figure 12. Plots of experimental values of R_g/R_g^s versus λ for networks swollen in toluene-d_8 together with R_g/R_g^s for networks swollen in cyclohexane-d_{12}: (○) R_g/R_g^s (toluene-d_8), (●) R_g/R_g° (cyclohexane-d_{12}); a, $\bar{k}$ = 3.1; b, $\bar{k}$ = 4.1; c, $\bar{k}$ = 5.2.

Kratky plots of scattering from all networks show maxima as in Figure 5. This phenomenon was also found by Bastide et al.,[11] who have reported that this is qualitatively consistent with theoretical calculations on networks. Their result might apply to our systems, but this is uncertain. Their networks contained many cross-links per labeled chain, and ours contained only a few. The maxima they observed occurred at values of q substantially lower than found in our experiments. At higher q, a multiplicity of other effects make analysis of the experiment uncertain.

Maxima in Kratky plots in our experiments are found at values of q lying between 0.05 and 0.06 Å^{-1}. A Gaussian coil is a poor model in this range, since the characteristic distance q^{-1} is 15–20 Å. The thickness of the chain and the importance of the details of conformational structure may lead to $q^2I(\mathbf{q})$ increasing or decreasing with q. Examples of this have been reported on partially deuteriated polystyrene[36] and in poly(methyl methacrylate).[37] Accordingly, while it may be proper to apply the analysis of Bastide et al.[11] to our system, we are reluctant to draw any conclusions about the deviation of our Kratky plots from that found for normal Gaussian molecules in the absence of network forces.

The maxima in plots of $I(\mathbf{q})$ versus q for PSH networks in toluene-d_8 shown in Figure 6 is characteristic of a "correlation hole" which has been found in other studies of polymer networks.[38] It is indicative of regions in space where the mean polymer concentration is greater or less than the overall mean. Presumably these regions are centered at cross-link junctions. Davidson and Richards, who have studied similar systems, have not reported such a phenomenon,[39] perhaps because their experiments were not performed over a wide enough range of q.

One of the motives in performing the SANS experiments of PSD/PSH gels swollen in cyclohexane was to ascertain whether an unusual result of Davidson and Richards[39] would be observed in our networks. They found that R_g of fully swollen gels in cyclohexane increased to a maximum and then decreased with increasing temperature. This decrease in R_g took place even though the degree of swelling continued to increase. As can be seen from Table II and parts a through c of Figure 9, this did not occur in our networks, in which R_g is seen to increase monotonically and smoothly with λ.

Uniaxially Stretched Networks. The SANS experiments on swollen gels are marred by the uncertainty of a proper reference state. This does not occur for a stretched bulk polymer. The results from Table III are compared with theoretical calculations in parts a–c of Figure 11. Two characteristics are evident. First of all theoretical curves of $R_\parallel/R_g^\circ$ for both the fixed junction and phantom network are concave upward as a function of λ, but our data are concave downward. The Flory–Erman model in certain ranges of deformation is also concave downward. According to their reasoning this arises from increasing fluctuations parallel to the stretching direction with increasing elongation. We note that our experiments do agree with their theory here. The experiments on $R_\perp/R_g^\circ$ should, according to Flory and Erman, approach the fixed junction model at higher elongation. Our results are unclear because $R_\perp/R_g^\circ$ is close to unity, and effects are partially obscured by experimental errors. In general, uniaxially stretched networks deform more than indicated by the phantom network and less than given by the fixed junction model. This also is consistent with the Flory–Erman model in a general way.

Kratky plots of the stretched samples (Figure 7) exhibit a broad maximum similar to that found for the swollen gels. This is consistent with predictions of Bastide et al.[11] though as we have pointed out earlier, those predictions may not apply to our system.

Among many uncertainties in studies of networks cross-linked from a liquid polymer or polymer solution is the possibility that portions of the network formed in the early stages of cross-linking are structurally distinct from that formed in latter stages of reaction. This might come about in the following way. In the early stages of cross-linking, the gel fraction can contract and squeeze out uncross-linked and soluble cross-linked chains. This decreases the extent of chain entanglement in those portions of the network that are formed near the onset of cross-linking. This process is less likely as the cross-linking reaction proceeds. A possible result is the formation of large scale inhomogeneities based on whether network formation was in the early or late stage of cross-linking. If true, it is possible that the interpretation of SANS experiments by many researchers including ourselves contains as yet unknown errors. Some recent studies of Soni and Stein[40] have given force to these suspicions.

Acknowledgment. We are grateful to Professors J. S. King and G. C. Summerfield for support and advice throughout the study. Kenneth Mazich of the Ford Motor Co. guided and worked with us in the preparation of the uniaxially oriented samples. Keith Shaw of the Biophysics Research Institute advised us and carried out FTIR measurements used in sol–gel analysis. Dr. G. D. Wignall

of the National Center for Small Angle Scattering Research (NCSASR) at Oak Ridge provided direction and guidance in carrying out the scattering experiments. Linda Maddox of NCSASR provided the code for the ELLIPSE method of analyzing stretched specimens. The National Science Foundation supported the research with Grand DMR-8217460.

Registry No. (BDSA)(S) (copolymer), 115464-50-1; neutron, 12586-31-1.

References and Notes

(1) Kuhn, W. *Kolloid-Z.* **1936**, *76*, 258.
(2) Treloar, L. R. G. *Trans. Faraday Soc.* **1943**, *39*, 36.
(3) James, H. M.; Guth, E. *J. Chem. Phys.* **1947**, *15*, 651.
(4) James, H. M.; Guth, E. *J. Chem. Phys.* **1947**, *15*, 669.
(5) Flory, P. J. *Proc. R. Soc. London, A* **1976**, *A351*, 351.
(6) Deam, R. T.; Edwards, S. F. *Philos. Trans. R. Soc. London, A* **1976**, *A280*, 1296.
(7) Flory, P. J. *J. Chem. Phys.* **1977**, *66*, 5720.
(8) Erman, B.; Flory, P. J. *Macromolecules* **1982**, *15*, 806.
(9) Erman, B. *Macromolecules* **1987**, *20*, 1917.
(10) Bastide, J.; Picot, C.; Candau, S. J. *J. Macromol. Sci., Phys.* **1981**, *B19*, 13.
(11) Bastide, J.; Herz, J.; Boue, F. *J. Phys. (Les Ulis, Fr.)* **1985**, *46*, 1967.
(12) Ullman, R. *Macromolecules* **1982**, *15*, 582.
(13) Ullman, R. In *Elastomers and Rubber Elasticity*; Mark, J. E., Lal, J., Eds.; ACS Symposium Series 193; American Chemical Society: Washington, DC, 1982; Chapter 14.
(14) Beltzung, M.; Herz, J.; Picot, C. *Macromolecules* **1983**, *16*, 580.
(15) Williams, C.; Nierlich, M.; Cotton, J. P.; Jannink, G.; Boue, F.; Daoud, M.; Farnoux, B.; Picot, C.; de Gennes, P. G.; Rinaudo, M.; Mohan, M.; Wolff, C. *J. Polym. Sci., Polym. Lett. Ed.* **1979**, *17*, 370.
(16) Akcasu, A. Z.; Summerfield, G. C.; Jahshan, S. N.; Han, C. C.; Kim, C. Y.; Yu, H. *J. Polym. Sci., Polym. Phys. Ed.* **1980**, *18*, 863.
(17) Benoit, H.; Koberstein, J.; Leibler, L. *Makromol. Chem., Suppl.* **1981**, *4*, 85.
(18) Ullman, R. *J. Chem. Phys.* **1979**, *71*, 436.
(19) Ullman, R. *Macromolecules* **1982**, *15*, 1395.
(20) Edwards, S. F. *Proc. Phys. Soc., London* **1966**, *88*, 265.
(21) Dermer, O. C.; Edmison, M. T. *J. Am. Chem. Soc.* **1955**, *77*, 70.
(22) Heacock, J. F.; Edmison, M. T. *J. Am. Chem. Soc.* **1960**, *82*, 3460.
(23) Abramovitch, R. A.; Knaus, G. N.; Uma, V. *J. Org. Chem.* **1974**, *8*, 1101.
(24) Breslow, D. S.; Sloan, M. F.; Newburg, N. R.; Renfrow, W. B. *J. Am. Chem. Soc.* **1969**, *91*, 2273.
(25) Charlesby, A. *Proc. R. Soc. London, A* **1954**, *A222*, 542.
(26) Ullman, R. *J. Polym. Sci., Polym. Lett. Ed.* **1983**, *21*, 521.
(27) Ullman, R. *J. Polym. Sci., Polym. Phys. Ed.* **1984**, *23*, 1477.
(28) Summerfield, G. C.; Mildner, D. F. R. *J. Appl. Crystallogr.* **1983**, *16*, 384.
(29) Reynolds, L. E.; Mildner, D. F. R. *J. Appl. Crystallogr.* **1984**, *17*, 411.
(30) Wignall, G. D.; Bates, F. S. *J. Appl. Crystallogr.* **1987**, *20*, 28.
(31) King, J. S.; Boyer, W.; Wignall, G. D.; Ullman, R. *Macromolecules* **1985**, *18*, 709.
(32) Bauer, D. R.; Ullman, R. *Macromolecules* **1980**, *13*, 709.
(33) Strazielle, C.; Benoit, H. *Macromolecules* **1975**, *8*, 203.
(34) Daoud, M.; Cotton, J. P.; Farnoux, B.; Jannink, G.; Sarma, G.; Benoit, H.; Duplessix, R.; Picot, C.; de Gennes, P. G. *Macromolecules* **1975**, *8*, 704.
(35) Wiltzius, P.; Haller, H. R.; Cannell, D. S.; Schaefer, D. W. *Phys. Rev. Lett.* **1983**, *51*, 1183.
(36) Rawiso, M.; Duplessix, R.; Picot, C. *Macromolecules* **1987**, *20*, 630.
(37) O'Reilly, J. M.; Teegarden, D. M.; Wignall, G. D. *Macromolecules* **1985**, *18*, 2747.
(38) Benoit, H.; Decker, D.; Duplessix, R.; Picot, C.; Rempp, P.; Cotton, J. P.; Farnoux, B.; Jannink, G.; Ober, R. *J. Polym. Sci., Polym. Phys. Ed.* **1976**, *14*, 2119.
(39) Davidson, N. S.; Richards, R. W. *Macromolecules* **1986**, *19*, 2576.
(40) Soni, V.; Stein, R. S., private communication. Soni, V. Ph.D. Dissertation, University of Massachusetts, 1986.

Equilibrium Morphology of Block Copolymer Melts. 2

Kyozi Kawasaki, Takao Ohta,* and Mitsuharu Kohrogui

Department of Physics, Faculty of Science, Kyushu University 33, Fukuoka 812, Japan.
Received October 8, 1987

ABSTRACT: Our earlier theory on the same subject (Ohta, T.; Kawasaki, K. *Macromolecules*, **1986**, *19*, 2621) was reformulated so as to exhibit the scaling behavior inherent in the free energy functional. In this way we naturally recover the domain size of mesophases behaving as the two-thirds power of the polymerization index. The higher order long-range interactions of the parameter field are found not to be small and indicate a need to accurately calculate free energies in various mesophases, which is a purely geometrical problem in the strong segregation limit of the symmetric block copolymer model.

1. Introduction

In the previous paper to be referred to as part 1 on the same subject[1] we developed a theory of equilibrium morphology of block copolymer melts on the basis of Leibler's field-theoretic formulation.[2] There we have shown that effects of connectedness of the two blocks can be represented by repulsive (attractive) Coulomb-type forces between the monomers of the same (different) species. Here the main approximation for the model was that the part of the free-energy functional containing the long-range interaction of the local monomer concentration fluctuation can be represented by the above-mentioned Coulomb-type two-body interactions where we have seen cancellation of leading terms of the higher order interactions of long range. However, effects of the terms left out are yet to be examined. Indeed we will find that these terms are by no means negligible.

Another significant result which was found but was not stressed in part 1 is that in the strong segregation limit the dimensionless relative free energies of various mesophases are functions of the volume fraction of the A-rich domains uniquely determined by the geometry of the mesophase structures. Thus it is interesting to see how general this result is beyond the specific approximation made in part 1.

Under this circumstance we here reformulate the problem of equilibrium morphology of a block copolymer melt. Although we start in section 2 with the field-theoretic formalism as in part 1 and in Leibler's work, we do not rely on the mean-field approximation from the outset to derive the free-energy functional. The mean-field approximation will be replaced by certain assumptions like that associated

* Address correspondence to this author at the Department of Physics, Ochanomizu University, Tokyo 112, Japan.

0024-9297/88/2221-2972$01.50/0